

10

Permittivity Measurement

10.1	Measurement of Complex Permittivity at Low Frequencies	10-4
10.2	Measurement of Complex Permittivity Using Distributed Circuits	10-8
	Resonant Cavity Method • Free-Space Method for Measurement of Complex Permittivity • A Nondestructive Method for Measuring the Complex Permittivity of Materials	

Devendra K. Misra
University of Wisconsin

Dielectric materials possess relatively few free charge carriers. Most of the charge carriers are bound and cannot participate in conduction. However, these bound charges can be displaced by applying an external electric field. In such cases, the atom or molecule forms an electric dipole that maintains an electric field. Consequently, each volume element of the material behaves as an electric dipole. The dipole field tends to oppose the applied field. Dielectric materials that exhibit nonzero distribution of such bound charge separations are said to be *polarized*. The volume density of those electric dipoles is described by the volume density of polarization, \vec{P} . When a material is linear and isotropic in nature, the polarization density is related to applied electric field intensity, \vec{E} , as follows:

$$\vec{P} = \epsilon_0 \chi_e \vec{E} \quad (10.1)$$

where ϵ_0 ($= 8.854 \times 10^{-12}$ farad per meter) is the permittivity of free-space and χ_e is called the electric susceptibility of the material.

The electric flux density or displacement, \vec{D} , is defined as follows:

$$\vec{D} = \epsilon_0 \vec{E} + \vec{P} = \epsilon_0 (1 + \chi_e) \vec{E} = \epsilon_0 \epsilon_r \vec{E} = \epsilon \vec{E} \quad (10.2)$$

where ϵ is called the permittivity of the material and ϵ_r is its relative permittivity or dielectric constant. Electric flux density is expressed in Coulombs per square meter.

Equation 10.2 represents a relation between the electric flux density and the electric field intensity in the frequency domain. It will hold in time-domain only if the permittivity is independent of frequency. A material is called *dispersive* if its characteristics are frequency dependent. The product relation of Equation 10.2 in frequency domain will be replaced by a convolution integral for the time-domain fields.

Assuming that the fields are time-harmonic as $e^{j\omega t}$, the generalized Ampere's law can be expressed in phasor form as follows:

$$\nabla \times \vec{H} = \vec{J}^c + \vec{J} + j\omega \vec{D} \quad (10.3)$$

where H is the magnetic field intensity in Amperes per meter and J^e is the current-source density in Amperes per square meter. J is the conduction current density in Amperes per square meter, and the last term represents the displacement current density. J^e will be zero for a source-free region.

The conduction current density is related to the electric field intensity through Ohm's law as follows.

$$\vec{J} = \sigma \vec{E} \quad (10.4)$$

where σ is the conductivity of material in siemens per meter.

From Equations 10.2 to 10.4, we have,

$$\nabla \times \vec{H} = \vec{J}^e + \sigma \vec{E} + j\omega \epsilon \vec{E} \quad (10.5)$$

Conduction current represents the loss of power. There is another source of loss in dielectric materials. When a time-harmonic electric field is applied, the dipoles flip constantly back and forth. Because the charge carriers have finite mass, the field must do work to move them and they may not respond instantaneously. This means that the polarization vector will lag behind the applied electric field. This factor shows up at high frequencies. Therefore, Equation 10.5 is modified as follows:

$$\nabla \times \vec{H} = \vec{J}^e + \sigma \vec{E} + \omega \kappa'' \vec{E} + j\omega \epsilon \vec{E} = \vec{J}^e + j\omega \left(\epsilon - j \frac{\sigma + \omega \kappa''}{\omega} \right) \vec{E} = \vec{J}^e + j\omega \epsilon^* \vec{E} \quad (10.6)$$

Complex relative permittivity of a material is defined as follows:

$$\epsilon_r^* = \frac{\epsilon^*}{\epsilon_0} = \frac{1}{\epsilon_0} \left(\epsilon - j \frac{\sigma + \omega \kappa''}{\omega} \right) = \epsilon_r' - j\epsilon_r'' = \epsilon_r' (1 - j \tan \delta) \quad (10.7)$$

where ϵ_r' and ϵ_r'' represent real and imaginary parts of the complex relative permittivity. The imaginary part is zero for a lossless material. The term $\tan \delta$ is called the *loss-tangent*. It represents the tangent of the angle between the displacement phasor and total current, as shown in Figure 10.1. Thus, it will be close to zero for a low-loss material. Dielectric characteristics of selected substances are given in [Tables 10.1](#) and [10.2](#).

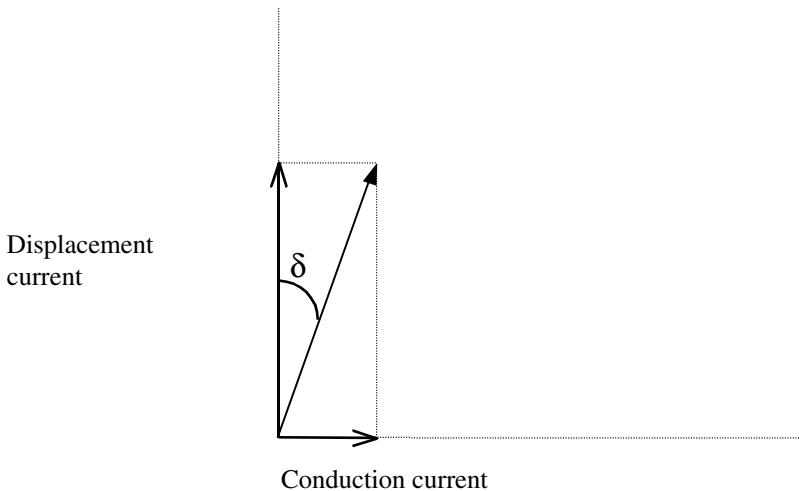


FIGURE 10.1 A phasor diagram representing displacement and loss currents.

TABLE 10.1 Complex Permittivity of Some Substances at Room Temperature

Substance	60 Hz	1 MHz	10 GHz
Nylon	3.60-j 0.06	3.14-j 0.07	2.80-j 0.03
Plexiglass	3.45-j 0.22	2.76-j 0.04	2.5-j 0.02
Polyethylene	2.26-j 0.0005	2.26-j 0.0005	2.26-j 0.0011
Polystyrene	2.55-j 0.0077	2.55-j 0.0077	2.54-j 0.0008
Styrofoam	1.03-j 0.0002	1.03-j 0.0002	1.03-j 0.0001
Teflon	2.1-j 0.01	2.1-j 0.01	2.1-j 0.0008
Glass (lead barium)	6.78-j 0.11	6.73-j 0.06	6.64-j 0.31

TABLE 10.2 Dielectric Properties of Biological Tissues at Selected Frequencies

	10 kHz		100 kHz		10 MHz		100 MHz		1 GHz	
	ϵ_r	σ' (S/m)	ϵ_r	σ' (S/m)	ϵ_r	σ' (S/m)	ϵ_r	σ' (S/m)	ϵ_r	σ' (S/m)
Brain (gray matter)	15×10^3	0.1	3000	0.14	300	0.3	90	0.7	60	1.2
Heart muscle	6×10^4	0.15	12×10^3	0.2	350	0.5	80	0.9	60	1.2
Kidney (cortex)	3×10^4	0.14	7000	0.2	350	0.6	85	1	60	1.5
Liver	2×10^4	0.05	7500	0.09	200	0.35	65	0.5	50	0.9
Lung (inflated)	9×10^3	0.07	2000	0.09	130	0.2	30	0.3	25	0.4
Spleen	12×10^3	0.1	3500	0.12	450	0.4	75	0.85	55	1.2
Uterus	2×10^4	0.5	2500	0.5	300	0.65	80	1	60	1.5
Skin	2×10^4	0.005	10^4	0.08	150	0.4	60	0.5	55	0.9

Source: Adapted from [9], $\sigma' = \sigma + \omega\kappa''$.

TABLE 10.3 Dielectric Dispersion Parameters for Some Liquids at Room Temperature

Substance	ϵ_∞	ϵ_s	α	τ (picoseconds)
Water	5	78	0	8.0789
Methanol	5.7	33.1	0	53.0516
Ethanol	4.2	24	0	127.8545
Acetone	1.9	21.2	0	3.3423
Ethylene glycol	3	37	0.23	79.5775
Propanol	3.2	19	0	291.7841
Butanol	2.95	17.1	0.08	477.4648
Chlorobenzene	2.35	5.63	0.04	10.2920

Dispersion characteristics of a large class of materials can be represented by the following empirical equation of Cole-Cole.

$$\epsilon_r^* = \epsilon_\infty + \frac{\epsilon_s - \epsilon_\infty}{1 + (j\omega\tau)^{1-\alpha}} \tag{10.8}$$

where ϵ_∞ and ϵ_s are the relative permittivities of material at infinite and zero frequencies, respectively. ω is the signal frequency in radians per second and τ is the characteristic relaxation time in seconds. For α equal to zero, Equation 10.8 reduces to the Debye equation. Dispersion parameters for a few liquids are given in Table 10.3.

Complex permittivity of a material is determined using lumped circuits at low frequencies, and distributed circuits or free-space reflection and transmission of waves at high frequencies. Capacitance and dissipation factor of a lumped capacitor are measured using a bridge or a resonant circuit. The complex permittivity is calculated from this data. At high frequencies, the sample is placed inside a

transmission line or a resonant cavity. Propagation constants of the transmission line or resonant frequency and the quality factor of the cavity resonator are used to calculate the complex permittivity. Propagation characteristics of electromagnetic waves are influenced by the complex permittivity of that medium. Therefore, a material can be characterized by monitoring the reflected and transmitted wave characteristics as well.

10.1 Measurement of Complex Permittivity at Low Frequencies [1,2]

A parallel-plate capacitor is used to determine the complex permittivity of dielectric sheets. For a separation d between the plates of area A in vacuum, the capacitance is given by

$$C_0 = 8.854 \frac{A}{d} \text{ pF} \quad (10.9)$$

where all dimensions are measured in meters. If the two plates have different areas, then the smaller one is used to determine C_0 . Further, it is assumed that the field distribution is uniform and perpendicular to the plates. Obviously, the fringing fields along the edges do not satisfy this condition. As shown in Figure 10.2, the guard electrodes are used to ensure that the field distribution is close to the assumed condition. For best results, the width of the guard electrode must be at least $2d$ and the unguarded plate must extend to the outer edge of the guard electrode. Further, the gap between the guarded and guard electrodes must be as small as possible.

The radius of guarded electrode is r_1 and the inner radius of guard electrode is r_2 . It is assumed that $R - r_2 \geq 2d$. The area A for this parallel plate capacitor is πr^2 , where r is defined as follows:

$$r = r_1 + \Delta \quad (10.10)$$

$$\Delta = \frac{1}{2}(r_2 - r_1) - \frac{2d}{\pi} \ln \left(\cosh \frac{\pi(r_2 - r_1)}{4d} \right) = \frac{1}{2}(r_2 - r_1) - 1.4659d \ln \left(\cosh 0.7854 \frac{r_2 - r_1}{d} \right) \quad (10.11)$$

Using the Debye model (i.e., $\alpha = 0$ in Equation 10.8), an equivalent circuit for a dielectric-filled parallel plate capacitor can be drawn as shown in Figure 10.3. If a step voltage V is applied to it, then the current I can be found as follows [2].

$$I = \epsilon_\infty C_0 V \delta(t) + \frac{VC_0(\epsilon_s - \epsilon_\infty)}{\tau} \exp\left(-\frac{t}{\tau}\right) \quad (10.12)$$

where $\tau = RC_0(\epsilon_s - \epsilon_\infty)$

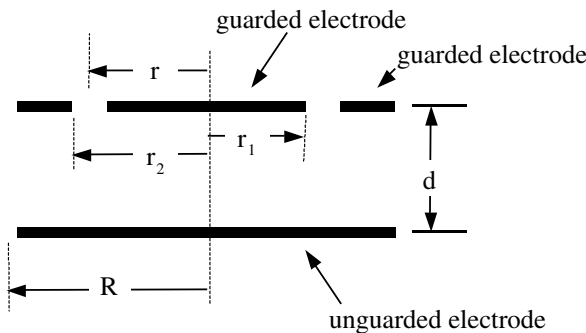


FIGURE 10.2 Geometry of a guarded capacitor.

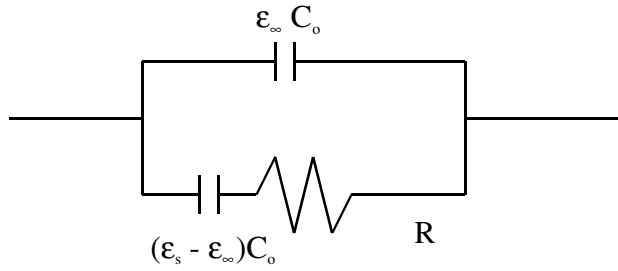


FIGURE 10.3 Equivalent circuit of a parallel-plate capacitor based on the Debye's model.

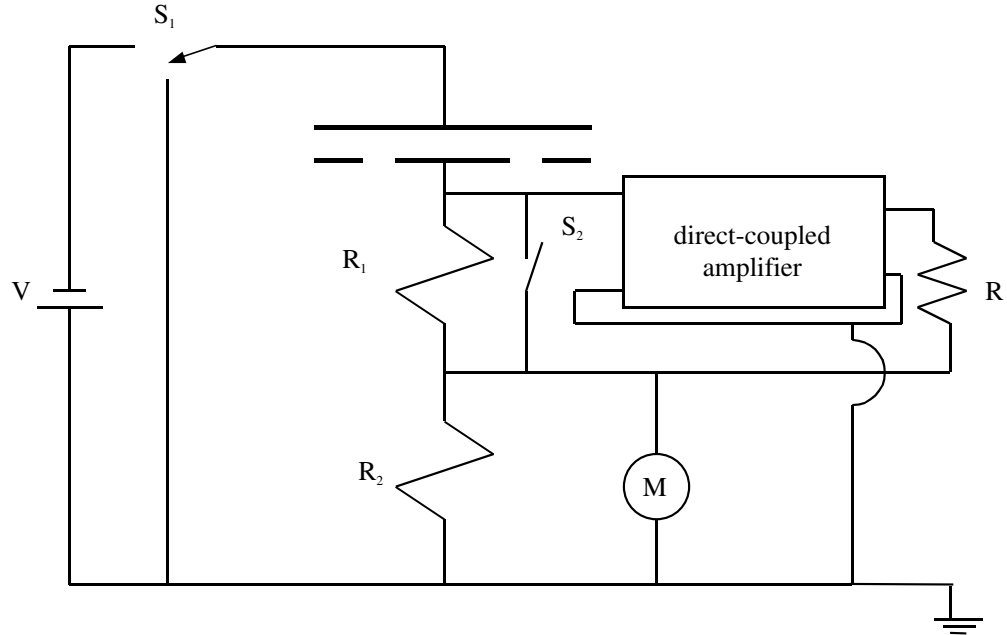


FIGURE 10.4 Circuit arrangement for the characterization of dielectric materials using a step voltage.

The first term in Equation 10.12 represents the charging current of capacitor $\epsilon_{\infty} C_0$ in the upper branch. This current is not measured because it disappears instantaneously. In practice, it needs to be bypassed briefly to protect the detector from overloading or burning. The second term of Equation 10.12 represents charging current of the lower branch of an equivalent circuit. The time constant, τ , is determined following the decay characteristics of this current. Further, the resistance R can be found after extrapolating this current-time curve to $t = 0$. The discharging current characteristics are used to remove V at $t = 0$.

A typical circuit arrangement for the characterization of dielectric materials using a step voltage is shown in Figure 10.4. A standard resistor R_1 of either 10^{10} or $10^{12} \Omega$ is connected between the guarded electrode and the load resistor R_2 . A feedback circuit is used that forces the voltage drop across R_1 to be equal in magnitude but opposite in polarity to that of across R_2 . It works as follows. Suppose that the node between capacitor and R_1 has a voltage V_1 with respect to the ground. It is amplified but reversed in polarity by the amplifier. Therefore, the current through R_1 will change. This process continues until the input to the amplifier is zero. The junction between R_1 and the capacitor will then be at the ground potential. Thus, the meter M measures voltage across R_2 that is negative of the voltage across R_1 . Since R_1 is known, the current through it can be calculated. This current also flows through the sample. S_1 is used to switch from the charging to discharging mode while S_2 is used to provide a path for surge currents.

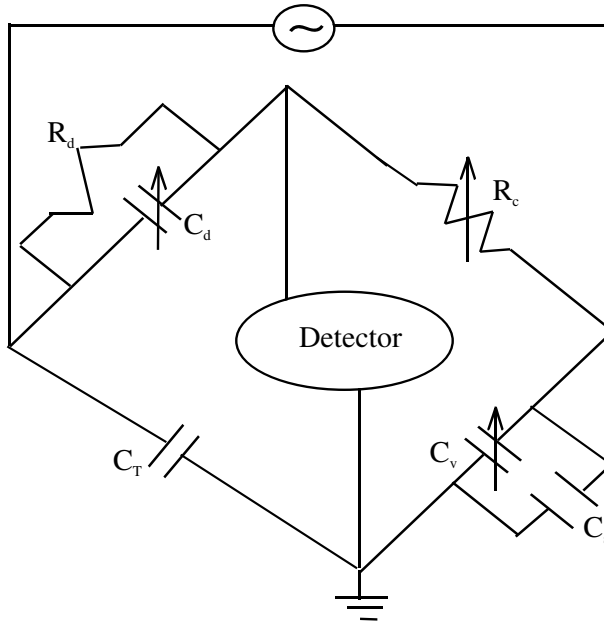


FIGURE 10.5 Schering bridge.

Capacitance and the dissipation factor of the dielectric-loaded parallel-plate capacitor are used in the medium frequency range to determine the complex permittivity of materials. A substitution method is generally employed in the Schering bridge circuit for this measurement.

In the Schering bridge shown in Figure 10.5, assume that the capacitor C_v is disconnected for the time being, and the capacitor C_s contains the dielectric sample. In case of a lossy dielectric sample, it can be modeled as an ideal capacitor C_x in series with a resistor R_x . The bridge is balanced by adjusting C_d and R_c . An analysis of this circuit under the balanced condition produces the following relations.

$$R_x = \frac{C_d R_c}{C_T} \quad (10.13)$$

and,

$$C_x = \frac{C_T R_d}{R_c} \quad (10.14)$$

Quality factor Q of a series RC circuit is defined as the tangent of its phase angle while the inverse of Q is known as the dissipation factor D . Hence,

$$Q = \frac{X_x}{R_x} = \frac{1}{\omega C_x R_x} = \frac{1}{D} \quad (10.15)$$

For a fixed R_d , the capacitor C_d can be calibrated directly in terms of the dissipation factor. Similarly, the resistor R_c can be used to determine C_x . However, an adjustable resistor limits the frequency range. A substitution method is preferred for precision measurement of C_x at higher frequencies. In this technique, a calibrated precision capacitor C_v is connected in parallel with C_s as shown in Figure 10.5 and the bridge is balanced. Assume that the settings of two capacitors at this condition are C_{d1} and C_{v1} . The capacitor C_s is then removed and the bridge is balanced again. Let the new settings of these capacitors

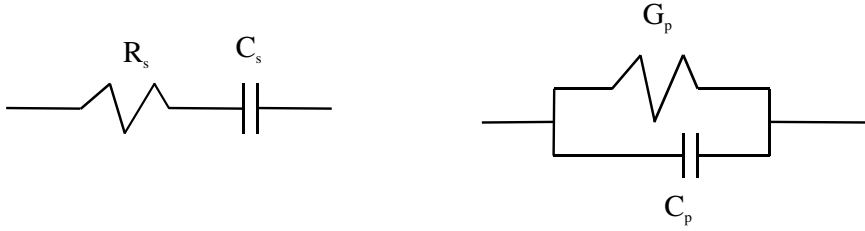


FIGURE 10.6 Series and parallel equivalent circuits of a dielectric-loaded capacitor.

be C_{d2} and C_{v2} , respectively. Equivalent circuit parameters of the dielectric-loaded capacitor C_s are then found as follows.

$$C_x = C_{v2} - C_{v1} \quad (10.16)$$

$$D_x = \frac{C_{v2}}{C_x} \delta D \quad (10.17)$$

where $\delta D = \omega R_d (C_{d1} - C_{d2})$.

Complex permittivity of the specimen is calculated from this data as follows:

$$\epsilon'_r = \frac{C_x}{C_0} \quad (10.18)$$

and,

$$\epsilon''_r = \frac{C_x D_x}{C_0} \quad (10.19)$$

So far, a series RC circuit equivalent model is used for the dielectric-loaded capacitor. As illustrated in Figure 10.6, an equivalent parallel RC model can also be obtained for it. The following equations can be used to switch back and forth between these two equivalent models.

$$G_p = \frac{R_s}{R_s^2 + \frac{1}{\omega^2 C_s^2}} = \frac{1}{R_s} \left(\frac{1}{1 + Q^2} \right) \quad (10.20)$$

$$C_p = \frac{C_s}{1 + (\omega R_s C_s)^2} = \frac{C_s}{1 + D^2} \quad (10.21)$$

$$R_s = \frac{G_p}{G_p^2 + \omega^2 C_p^2} = \frac{1}{G_p} \left(\frac{1}{1 + Q^2} \right) \quad (10.22)$$

$$C_s = \frac{G_p^2 + \omega^2 C_p^2}{\omega^2 C_p} = C_p (1 + D^2) \quad (10.23)$$

and,

$$Q = \frac{1}{D} = \frac{\omega C_p}{G_p} = \frac{1}{\omega R_s C_s} \quad (10.24)$$

Proper shielding and grounding arrangements are needed for a reliable measurement, especially at higher frequencies. Grounding and edge capacitances of the sample holder need to be taken into account for improved accuracy. Further, a guard point needs to be obtained that may require balancing in some cases. An inductive-ratio-arm capacitance bridge may be another alternative to consider for such applications [1].

10.2 Measurement of Complex Permittivity Using Distributed Circuits

Measurement techniques based on the lumped circuits are limited up to the lower end of VHF band. The characterization of materials at microwave frequencies requires the distributed circuits. A number of techniques have been developed on the basis of wave reflection and transmission characteristics inside a transmission line or in free-space. Some other methods employ a resonant cavity that is loaded with the sample. Cavity parameters are measured and the material characteristics are deduced from that. A number of these techniques are described in [3,4] that can be used for a sheet material. These techniques require cutting a piece of sample to be placed inside a transmission line or a cavity. In case of liquid or powder samples, a so-called modified infinite sample method can be used. In this technique, a waveguide termination is filled completely with the sample as shown in Figure 10.7. Since a tapered termination is embedded in the sample, the wave incident on it dissipates with negligible reflection and it looks like the sample is extending to infinity. The impedance at its input port depends on the electrical properties of filling sample. Its VSWR S and location of first minimum d from the load plane are measured using a slotted line. The complex permittivity of the sample is then calculated as follows [5].

$$\epsilon'_r = \left(\frac{\lambda}{\lambda_c}\right)^2 + \frac{\left[1 - \left(\frac{\lambda}{\lambda_c}\right)^2\right] \times \left[S^2 \sec^4(\beta d) - (1 - S^2)^2 \tan^2(\beta d)\right]}{\left[1 + S^2 \tan^2(\beta d)\right]^2} \quad (10.25)$$

and,

$$\epsilon''_r = \frac{\left[1 - \left(\frac{\lambda}{\lambda_c}\right)^2\right] \times \left[2S(1 - S^2)^2 \sec^4(\beta d) \tan(\beta d)\right]}{\left[1 + S^2 \tan^2(\beta d)\right]^2} \quad (10.26)$$

where λ is the free-space wavelength; λ_c is the cut-off wavelength for the mode of propagation in the empty guide, and β is the propagation constant in the feeding guide. It is assumed that the waveguide supports the TE_{10} mode only.

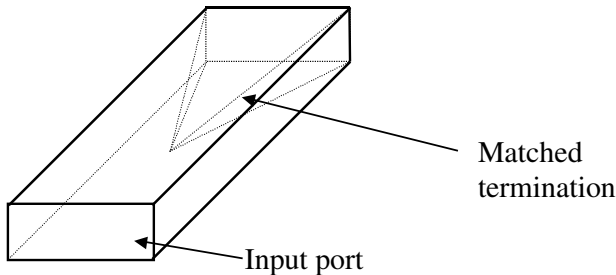


FIGURE 10.7 A waveguide termination filled with liquid or powder sample.

Resonant Cavity Method

A cavity resonator can be used to determine the complex permittivity of materials at microwave frequencies. If a cavity can be filled completely with the sample, then the following procedure can be used.

Measure the resonant frequency f_1 and the quality factor Q_1 of an empty cavity. Next, fill that cavity with the sample material and measure its new resonant frequency f_2 and quality factor Q_2 . The dielectric parameters of the sample are then calculated from the following formulas [3].

$$\epsilon_r = \left(1 + \frac{f_1 - f_2}{f_2} \right)^2 \quad (10.27)$$

and,

$$\tan \delta = \frac{1}{Q_2} - \frac{1}{Q_1} \sqrt{\frac{f_1}{f_2}} \quad (10.28)$$

On the other hand, a cavity perturbation technique will be useful for smaller samples [4]. If the sample is available in a circular cylindrical form, then it may be placed inside a TE_{101} rectangular cavity through the center of its broad face where the electric field is maximum. Its resonant frequency and quality factor with and without sample are then measured. The complex permittivity of the sample is calculated as follows.

$$\epsilon'_r = 1 + \frac{1}{2} \frac{f_1 - f_2}{f_2} \frac{V}{v} \quad (10.29)$$

and,

$$\epsilon''_r = \frac{V}{4v} \frac{Q_2 - Q_1}{Q_1 Q_2} \quad (10.30)$$

where V and v are cavity and sample volumes, respectively.

Similarly, for a small spherical sample of radius r that is placed in a uniform field at the center of the rectangular cavity, the dielectric parameters are found as follows.

$$\epsilon'_r = \frac{abd}{8\pi r^3} \frac{f_1 - f_2}{f_2} \quad (10.31)$$

and,

$$\epsilon''_r = \frac{abd}{16\pi r^3} \left(\frac{Q_2 - Q_1}{Q_1 Q_2} \right) \quad (10.32)$$

where a , b , and d are the width, height, and length of the rectangular cavity, respectively. For the highest accuracy with the cavity perturbation method, the shift in frequency ($f_1 - f_2$) must be very small.

Free-Space Method for Measurement of Complex Permittivity

When a plane electromagnetic wave is incident on a dielectric interface, its reflection and transmission depend upon the contrast in the dielectric parameters. Many researchers have used it for determining the complex permittivity of dielectric materials placed in free-space. An automatic network analyzer and phase-corrected horn antennas may be used for such measurements [6]. The system is calibrated using the TRL (through, reflect, and line) technique. A time-domain gating is used to minimize error due to multiple reflections. The sample of thickness d is placed in front of a conducting plane and its reflection coefficient S_{11} is measured. A theoretical expression for this reflection coefficient is found as follows.

$$S_{11} = \frac{jZ_d \tan(\beta_d d) - 1}{jZ_d \tan(\beta_d d) + 1} \quad (10.33)$$

where,

$$Z_d = \frac{1}{\sqrt{\epsilon_r^*}} \quad (10.34)$$

$$\beta_d = \frac{2\pi}{\lambda} \sqrt{\epsilon_r^*} \quad (10.35)$$

and λ is the free-space wavelength of electromagnetic signal.

Equation 10.33 is solved for ϵ_r^* after substituting the measured S_{11} . Since it represents a nonlinear relation, an iterative numerical procedure may be used.

A Nondestructive Method for Measuring the Complex Permittivity of Materials

Most of the techniques described so far require cutting and placing part of a sample in the test fixture. Sometimes it may not be permissible to do so. Further, the dielectric parameters may change in that process. It is especially important in the case of a biological specimen to perform *in vivo* measurements. In one such technique, an open-ended coaxial line is placed in close contact with the sample and its input reflection coefficient is measured using an automatic network analyzer [7,8]. Open-ended coaxial lines are used as sensors for *in situ* measurement of electrical properties of materials because they possess several advantages over others [9–13]. Besides its usefulness over a broad frequency band, coaxial probes require almost no preparation of samples [9,13]. Further, a needle-like coaxial probe can be inserted easily into the sample for *in vivo* characterization of materials [11]. As recommended by the manufacturers, the network analyzer is calibrated initially using an open circuit, a short circuit, and a matched load. The reference plane is then moved to the measuring end of the coaxial line using a short circuit. Electrical parameters of the material are extracted subsequently via a suitable admittance model of the coaxial opening [12]. If the coaxial opening is electrically small such that its radiation fields are negligible and the sample volume is large enough to contain the aperture fields in it, then a significantly simple procedure can be adopted. This does not require the usual calibration of the network analyzer and shifting of the reference plane. It utilizes four standards (materials of known electrical properties) to calibrate the measurement setup. Typically, an open circuit, a short circuit, and two different materials of known electrical characteristics are used in this technique. Since this procedure is not based on the manufacturer's recommended calibration (does not require exact reflection coefficient data), a reflectometer arrangement with amplitude and phase measurement options can produce fairly accurate results [14]. One such arrangement is illustrated in Figure 10.8. The procedure is summarized below.

One end of the coaxial line is connected to the automatic network analyzer and the other is left open in the air. The reflection coefficient for this case is recorded as Γ_1 . Next, the probe is dipped in distilled water and then in methanol, and the corresponding reflection coefficients are recorded as Γ_2 and Γ_4 , respectively. With aluminum foil pressed against the opening, its reflection coefficient is recorded as Γ_3 . These four measurements are used to calibrate the system. Now, a coefficient ξ is computed as follows:

$$\xi = \frac{(1+\Delta)\epsilon_{r4}^* - \epsilon_{r1}^* - \epsilon_{r2}^*\Delta}{\epsilon_{r1}^{*2} + \epsilon_{r2}^{*2}\Delta - (1+\Delta)\epsilon_{r4}^{*2}} \quad (10.36)$$

where ϵ_{r1}^* , ϵ_{r2}^* , and ϵ_{r4}^* are complex relative permittivities of air, water, and methanol at the frequency of measurement, and

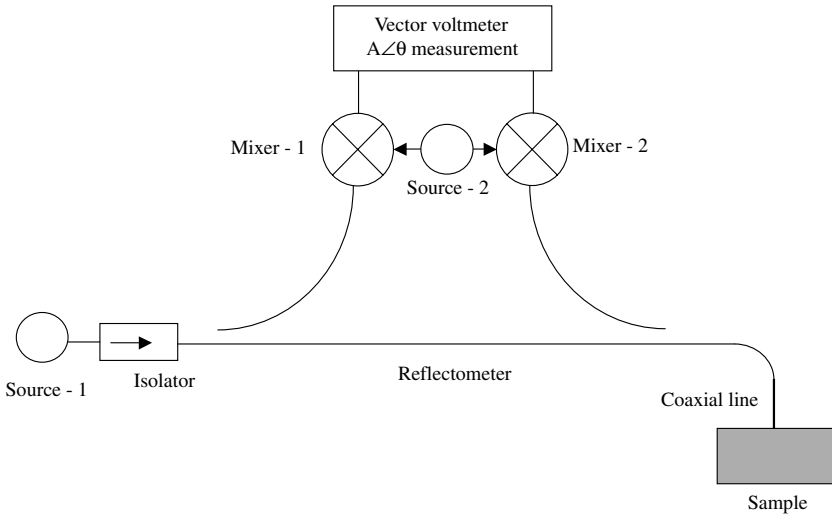


FIGURE 10.8 A reflectometer arrangement for measuring the complex permittivity of materials using a coaxial probe.

$$\Delta = \frac{(\Gamma_4 - \Gamma_1) \times (\Gamma_3 - \Gamma_2)}{(\Gamma_4 - \Gamma_2) \times (\Gamma_1 - \Gamma_3)} \quad (10.37)$$

It should be noted that the magnitudes of these reflection coefficients $|\Gamma_i|$ may occasionally exceed unity because the measurement system is not calibrated for this.

The equivalent admittance parameter (dimensionless) at the aperture is represented by

$$y = \epsilon_r^* + \zeta \epsilon_r^{*2} \quad (10.38)$$

Note that y is not exactly the admittance of the aperture that is terminated by a material of complex relative permittivity ϵ_r^* . The parameters y_1 and y_2 are determined via this equation using ϵ_{r1}^* and ϵ_{r2}^* respectively.

Next, repeating the measurement with the sample material, the reflection coefficient is recorded as Γ_s . The aperture-admittance parameter with the sample is then computed as follows:

$$y_s = \frac{y_1 - \xi y_2}{1 - \xi} \quad (10.39)$$

where,

$$\xi = \frac{(\Gamma_s - \Gamma_1) \times (\Gamma_3 - \Gamma_2)}{(\Gamma_s - \Gamma_2) \times (\Gamma_1 - \Gamma_3)} \quad (10.40)$$

The complex permittivity ϵ_{rs}^* of the sample is determined from Equations 10.38 and 10.39 as follows:

$$\epsilon_{rs}^* = \frac{-1 \pm \sqrt{1 + 4 y_s \zeta}}{2 \zeta} \quad (10.41)$$

Only one of the solutions to Equation 10.41 is found to be a physically possible value because the real part of the complex permittivity must be a positive number and its imaginary part must be negative (the formulation is based on the time-harmonic representation of $e^{j\omega t}$).

References

- [1] A.R. Von Hippel, *Dielectric Materials and Applications*, The M.I.T. Press, Cambridge, MA, 1961.
- [2] N.E. Hill, W.E. Vaughan, A.H. Price, and M. Davies, *Dielectric Properties and Molecular Behaviour*, Van Nostrand Reinhold Co., London, 1969.
- [3] H. Altschuler, Dielectric constant, in *Handbook of Microwave Measurements*, Vol. II, M. Sucher and J. Fox, Eds., Polytechnic Press, Brooklyn, NY, 1963.
- [4] R. Chatterjee, *Advanced Microwave Engineering*, Ellis Horwood Ltd., Chichester, 1988.
- [5] D.K. Misra, Permittivity measurement of modified infinite samples by a directional coupler and a sliding load, *IEEE Trans. Microwave Theory Tech.*, 29(1), 65–67, 1981.
- [6] D.K. Ghodgaonkar, V.V. Varadan, and V.K. Varadan, A free-space method for measurement of dielectric constants and loss tangents at microwave frequencies, *IEEE Trans. Instrum. Meas.*, 38(3), 789–793, 1989.
- [7] A.P. Gregory, R.N. Clarke, T.E. Hodgetts, and G.T. Symm, RF and microwave dielectric measurements upon layered materials using a reflectometric coaxial sensor, NPL Report DES 125, UK, March 1993.
- [8] D. Misra, On the measurement of the complex permittivity of materials by an open-ended coaxial probe, *IEEE Microwave Guided Wave Lett.*, 5(5), 161–163, 1995.
- [9] S. Gabriel, R.W. Lau, and C. Gabriel, The dielectric properties of biological tissues: II. Measurements in the frequency range 10 Hz to 20 GHz, *Phys. Med. Biol.*, 41, 2251–2269, 1996.
- [10] M.F. Kabir, K.B. Khalid, W.M. Daud, and S. Aziz, Dielectric properties of rubber wood at microwave frequencies measured with an open-ended coaxial line, *Wood Fiber Sci.*, 29(4), 319–324, 1997.
- [11] Y. Xu, R.G. Bosisio, A. Bonincontro, F. Pedone, and G.F. Mariutti, On the measurement of microwave permittivity of biological samples using needle-type coaxial probes, *IEEE Trans. Instrum. Meas.*, IM-42(4), 822–827, 1993.
- [12] C.L. Pournaropoulos and D.K. Misra, The coaxial aperture electromagnetic sensor and its application in material characterization, *Meas. Sci. Technol.*, 8, 1191–1202, 1997.
- [13] H.C.F. Martens, Reedijk, and H.B. Brom, Measurement of the complex dielectric constant down to helium temperatures. I. Reflection method from 1 MHz to 20 GHz using an open-ended coaxial line, *Rev. Scientific Instrum.*, 71(2), 473–477, 2000.
- [14] S.D. Zandron, C. Pournaropoulos, and D.K. Misra, Complex permittivity measurement of materials by the open-ended coaxial probe technique, *J. Wave-Mater. Interact.*, 5 & 6(4), 329–342, 1991.